

CRATER DETECTION ALGORITHMS BASED ON PREWITT, ABDU, ARGYLE, MACLEOD, DERIVATIVE-OF-GAUSSIAN AND CANNY GRADIENT EDGE DETECTORS. H. Knežević¹, G. Salamunićcar^{1,2,3} and S. Lončarić³, ¹Polytechnic of Zagreb, Vrbik 8A, HR-10000 Zagreb, Croatia, gen@inet.hr, ²AVL-AST d.o.o., Av. Dubrovnik 10/II, HR-10020 Zagreb-Novı Zagreb, Croatia, gsc@ieee.org, ³Faculty of Electrical Engineering and Computing, University of Zagreb, Unska 3, HR-10000 Zagreb, Croatia, sven.loncaric@fer.hr.

Summary: Implementations of six different Crater Detection Algorithms (CDA) based on six different well-known gradient edge detectors are presented. They were analyzed and compared using the Framework for Evaluation of CDAs (FECDA).

Introduction: CDAs' applications range from dating planetary surfaces [1] to advanced statistical analysis [2]. Overview of a large body of CDA-related literature as well as FECDA is given in [3]. In the previous work [4, 5, 6], six CDAs were implemented based on Radon/Hough transform (RH) and following gradient edge detectors: (1) Pixel-Difference; (2) Separated-Pixel-Difference; (3) Roberts; (4) Prewitt; (5) Sobel; and (6) Frei-Chen. In this work, six new CDAs were (re)implemented based on RH and following gradient edge detectors: (1) Prewitt (reimplementation) [7, 12]; (2) Abdou (new CDA) [8, 12]; (3) Argyle (new CDA) [9, 12]; (4) Macleod (new CDA) [10, 12]; (5) Derivative-Of-Gaussian or shortly DroG (new CDA) [12]; and (6) Canny (new CDA) [11, 12].

Methods: As shown in Table 1, used gradient edge detectors differ in used gradient masks. They also differ in correction factor f which can be computed from the masks. Argyle, Macleod, DroG and Canny are additionally different by using Gauss function to dynamically compute masks' elements for defined kernel, as given in Eqs 1. to 4. It can also be noticed that DroG and Canny have identical masks. Canny is additionally different by using non-maximum suppression and hysteresis-based thresholding. These two techniques were

turned off for all other CDAs, so that the original implementation of these operators can be properly compared with the Canny one.

$$G(x, \sigma) = \frac{1}{\sigma \cdot \sqrt{2 \cdot \pi}} \cdot e^{-\frac{x^2}{2 \cdot \sigma^2}} \quad (1)$$

$$\text{Argyle}(x, y, \sigma) = s \cdot G(x, \sigma) \cdot G(y, \sigma) \begin{cases} x < 0, s = -1 \\ x = 0, s = 0 \\ x > 0, s = 1 \end{cases} \quad (2)$$

$$\text{Macleod}(x, y, \sigma) = (G(x - \sigma, \sigma) - G(x + \sigma, \sigma)) \cdot G(y, \sigma) \quad (3)$$

$$\text{DroG}(x, y, \sigma) = x \cdot G(x, \sigma) \cdot G(y, \sigma) \quad (4)$$

Results: The analysis using F-ROC and detected edges are shown in Fig. 1. For evaluation of the results, from FECDA [3] the following were used: (1) 1/64° MOLA data; (2) the GT catalogue with 17582 craters as the last official version; and (3) Topolyzer application.

Conclusion: CDA based on Canny is significantly better than all other CDAs presented here. Accordingly, for now Canny is the most promising choice for future work on CDAs based on edge detection. It can also be noticed when different masks were used for the same operator, that better results are obtained with the smaller masks. The larger masks shown their advantage during our experimentation only when radius range was

Table 1: Masks of used gradient edge detectors: (1) Prewitt; (2) Abdou; (3) Argyle (for $\sigma = 0.5$); (4) Macleod (for $\sigma = 0.5$, first and last 3 lines contains only 0-s); (5) DroG (for $\sigma = 0.5$); and (6) Canny (for $\sigma = 0.5$).

1)	$\begin{vmatrix} -1 & 0 & 1 \\ -1 & 0 & 1 \\ -1 & 0 & 1 \end{vmatrix}$	$\begin{vmatrix} \dots & 0 & 1 & 1 \\ \dots & 0 & 1 & 1 \\ \dots & 0 & 1 & 1 \end{vmatrix}$	$\begin{vmatrix} \dots & 0 & 1 & 1 & 1 \\ \dots & 0 & 1 & 1 & 1 \\ \dots & 0 & 1 & 1 & 1 \end{vmatrix}$	2)	$\begin{vmatrix} -1 & -1 & 0 & 1 & 1 \\ -1 & -2 & 0 & 2 & 1 \\ -1 & -2 & 0 & 2 & 1 \\ -1 & -2 & 0 & 2 & 1 \\ -1 & -1 & 0 & 1 & 1 \end{vmatrix}$	$\begin{vmatrix} \dots & 0 & 1 & 1 & 1 \\ \dots & 0 & 2 & 2 & 1 \\ \dots & 0 & 3 & 2 & 1 \\ \dots & 0 & 3 & 2 & 1 \\ \dots & 0 & 3 & 2 & 1 \end{vmatrix}$	$\begin{vmatrix} \dots & 0 & 1 & 1 & 1 & 1 \\ \dots & 0 & 2 & 2 & 2 & 1 \\ \dots & 0 & 3 & 3 & 2 & 1 \\ \dots & 0 & 4 & 3 & 2 & 1 \\ \dots & 0 & 4 & 3 & 2 & 1 \\ \dots & 0 & 4 & 3 & 2 & 1 \\ \dots & 0 & 3 & 3 & 2 & 1 \\ \dots & 0 & 2 & 2 & 2 & 1 \\ \dots & 0 & 1 & 1 & 1 & 1 \end{vmatrix}$
3)	$\begin{vmatrix} \dots & 0000 & 0003 & 0000 \\ \dots & 0000 & 1353 & 0003 \\ \dots & 0000 & 9999 & 0025 \\ \dots & 0000 & 1353 & 0003 \\ \dots & 0000 & 0003 & 0000 \end{vmatrix}$	4)	$\begin{vmatrix} \dots & 0000 & 0003 & 0002 & 0001 & 0000 & 0000 \\ \dots & 0000 & 1353 & 0932 & 0211 & 0017 & 0001 \\ \dots & 0000 & 9999 & 6885 & 1561 & 0128 & 0004 \\ \dots & 0000 & 1353 & 0932 & 0211 & 0017 & 0001 \\ \dots & 0000 & 0003 & 0002 & 0001 & 0000 & 0000 \end{vmatrix}$	5)	$\begin{vmatrix} \dots & 0000 & 0003 & 0000 \\ \dots & 0000 & 1353 & 0007 \\ \dots & 0000 & 9999 & 0050 \\ \dots & 0000 & 1353 & 0007 \\ \dots & 0000 & 0003 & 0000 \end{vmatrix}$	6)	$\begin{vmatrix} \dots & 0000 & 0003 & 0000 \\ \dots & 0000 & 1353 & 0007 \\ \dots & 0000 & 9999 & 0050 \\ \dots & 0000 & 1353 & 0007 \\ \dots & 0000 & 0003 & 0000 \end{vmatrix}$

increased from 5~10 pixels to 40~80 pixels.

Acknowledgements: To colleague H. Novosel for initial implementation of Prewitt and Abdou edge detector, and to colleagues D. Gržanić, M. Karas, S. Katušić, M. Kovač, D. Mehić, D. Preloščan, N. Rizvanović, B. Spasić, Lj. Šare and D. Zorić for providing computers for the cluster which was used to achieve faster computation of optimal parameters for six different CDAs.

References: [1] Hartmann W. K. and Neukum G. (2001) *Space Science Reviews*, 96, 165-194. [2] Salamunićar G. (2004) *Adv. Space Res.*, 33, 2281-2287. [3] Salamunićar G. and Lončarić S. (in press) *Adv.*

Space Res., doi:10.1016/j.asr.2007.04.028. [4] Salamunićar G. and Lončarić S. (2006) *LPS XXXVII*, Abstract #1138. [5] Novosel H. et al. (2007) *LPS XXXVIII*, Abstract #1351. [6] Salamunićar G. and Lončarić S. (2007) *7th Int. Conf. on Mars*, Abstract #3066. [7] Prewitt J. (1970) in *Picture Processing and Psychopictories* (Lipkin B. and Rosenfeld A., Eds.), 75-149. [8] Abdou I. E. (1978) *USCIP Technical Report* 830, 95. [9] Argyle E. (1971) *Proc. IEEE*, 59, 285-286. [10] Macleod I. D. G. (1972) *Proc. IEEE*, 60, 344. [11] Canny J. F. (1986), *IEEE PAMI*, 8 (6), 679-698. [12] Pratt W. K. (2001) *Digital Image Processing*, John Wiley & Sons Inc., 443-508.

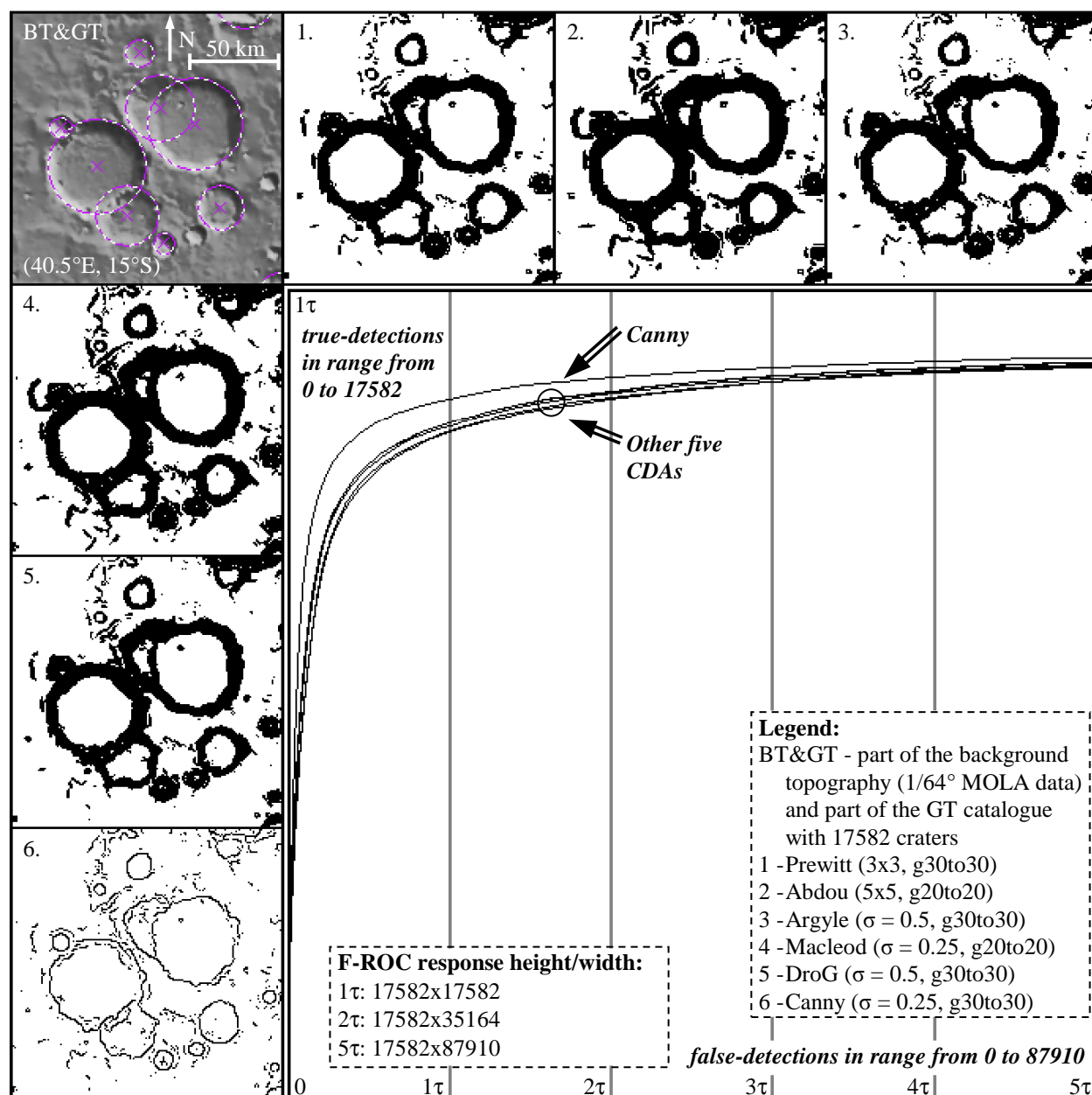


Figure 1: Detected edges (left and top) and F-ROC evaluations (right-bottom) for operators from Table 1.